Predicting Propeller Tonal noise with AI trained First-Principle Models: A Novel Methodology

Jatin Manghnani[1,2], Roland Ewert[2], Jan W. Delfs[2]

[1] *DLR, Innovation Center for Small Aircraft Technologies, 52146 Würselen-Aachen, Germany, Email: jatin.manghnani@dlr.de*

[2] *DLR, Institute of Aerodynamic and Flow Technology, 38108 Braunschweig, Germany*

Introduction

The development of energy-efficient, propeller-driven small aircraft and Advanced Air Mobility (AAM) vehicles faces challenges due to high noise levels, particularly in urban environments. This research proposes a reduced-order, data-driven semi-empirical model that combines physics-based and empirical approaches to predict tonal noise levels for isolated and installed propeller configurations. The model will integrate findings from computational aerodynamics (CA) and computational aeroacoustics (CAA) simulations at varying fidelity levels, along with empirical data from flight tests and wind tunnel experiments, to improve prediction accuracy. The framework involves selecting an appropriate propeller noise source model, validating it against measured flyover data, identifying key noise-influencing parameters, and training an artificial neural network (ANN) to capture complex relationships between inputs and noise levels. This integrated approach aims to reduce computational costs while improving the accuracy and efficiency of noise predictions, supporting informed design decisions for noise reduction in early development stages.

Propeller Noise Source Model

The development of a data-driven AI-trained reduced-order model necessitates the selection of an optimal propeller model, striking a balance between accuracy and computational efficiency. Among various options, we opted for the DLR's Unsteady Panel Method (UPM) [4], leveraging its ability to simulate unsteady aerodynamics at lower computational cost compared to conventional methods like unsteady RANS with actuator disc (URANS-AD). The UPM's design allows it to maintain the structure of the propeller wake for a longer duration, thanks to its absence of dissipation effects associated with refined volume grids. This property renders the vortex method an ideal choice for generating multiple simulations, essential for creating a large dataset for training an AI model.

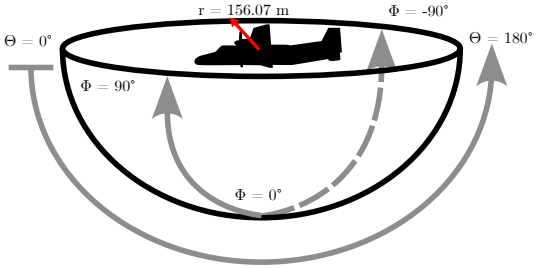

Figure 1: Representation of acoustic hemispherical far-field [1]

We employed Formulation 1A from F.Farassat [2], treating the propeller blade and wing geometry as the primary noise source under non-permeable surface assumptions. However, due to its first-principle based nature, the panel method code is unable to produce pressure fluctuations in the near-field associated with permeable surfaces, thus restricting its application to the propeller blades and wing surface. The loading on the blade and wing, represented by surface pressure, was used as input to the Ffowcs-William-Hawking (FW-H) equation for calculating loading noise. The volume of air displaced by the rotating propeller blade and moving wing generated pressure fluctuations, which in turn produced sound waves. This phenomenon is calculated using the thickness noise with spatial coordinates of the panels, discretized from the blade and wing geometry. The resulting time-domain noise signal was then converted to frequency domain using Fast Fourier Transform (FFT), representing the far-field acoustic radiation depicted in Fig. 1. A detailed explanation of the computational methodology deployed is provided by Manghnani *et al.* [1].

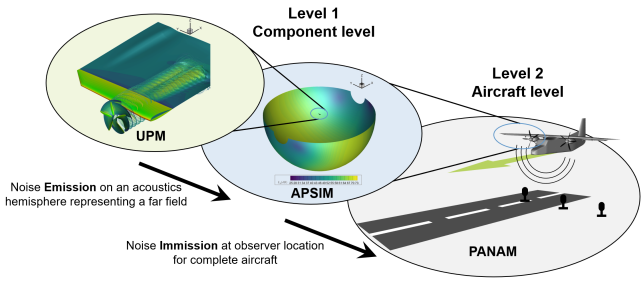

Figure 2: Computational Methodology [1]

The simulations was conducted for a half-wing installed with a single propeller, requiring validation for the full aircraft. APSIM-generated hemisphere data is processed in DLR's parametric aircraft noise analysis module, PANAM [6], which adds 3 dB to account for the second propeller and wing half. An additional 6 dB is included to account for ground reflection effects, as the microphone was ground based, plate-mounted [5]. Finally, Doppler effects are incorporated, and the results are compared to measurements. This methodology enables efficient dataset generation for AI training while ensuring realistic noise predictions. The complete computational framework is illustrated in Fig. 2.

Verification with BEMT-Hanson coupling

The noise levels on an acoustic hemisphere for an isolated propeller configuration are verified using BEMT-

Hanson coupling [7, 1]. The directivity of noise levels is plotted for both formulation-1A of APSIM and the Hanson model on an acoustic hemisphere with a radius of 156.07 m. The results demonstrate symmetry in azimuthal direction (Φ) for both cases, with the SPL values obtained using formulation 1A (FW-H) in APSIM closely matching those determined by the Hanson model. However, interfering patterns are observed in Farassat 1A result due to the larger step size used in aerodynamic simulations, which leads to interfering effects at extreme ends of the hemisphere, as depicted in Fig. 3.

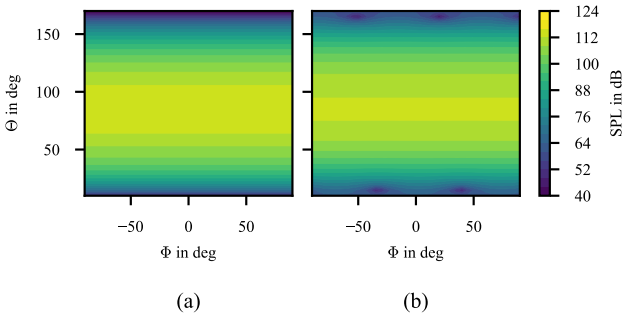

Figure 3: Noise directivity on acoustic hemispherical far-field (a) Hanson model [7], (b) Farassat 1A [3]

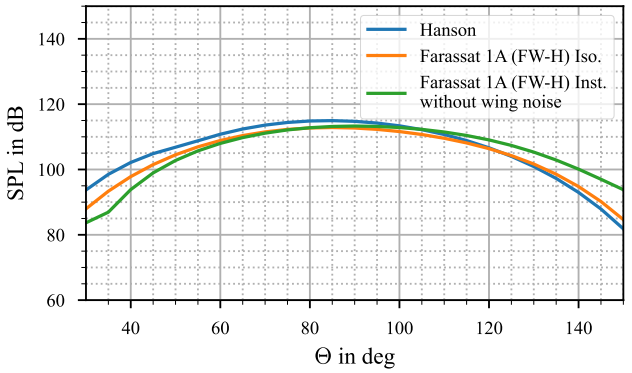

Figure 4: Noise directivity in polar coordinates at azimuth angle ($\Phi = 0°$)

The polar noise directivity at azimuthal angle $\Phi = 0°$ is also plotted in Fig. 4 for three cases: isolated propeller configurations using Hanson and APSIM, and installed propeller without wing in the CAA simulation using APSIM. The results indicate a difference in SPL values between Hanson and APSIM of 1 dB to 2 dB, which increases to 3 dB to 5 dB towards the hemisphere's extreme for isolated propeller configurations. Notably, the installed propeller configuration with the wing excluded from the CAA simulation exhibits a larger difference of 10 dB to 12 dB at the hemisphere's extreme due to backloading effects from the wing onto the propeller, as shown in Fig. 4.

Validation using DO-228 fly-over data

The noise levels obtained from isolated and installed propeller configurations are validated using data from DO-228 fly-over measurements [5]. For the installed configuration, two vortex methods - Vortex Filament Method (VFM) and Vortex Particle Method (VPM) - are employed to model the propeller wake. In VFM, a quad wake filament is utilized with a vortex core defined on lateral and longitudinal filaments [4], whereas in VPM, particles are used to represent the propeller wake with a vortex core assigned to each particle. The results for both methods were compared to the measured data from DO-228 fly-over measurements in two plots: non-weighted level time history and A-weighted spectrum, as depicted in Fig. 5.

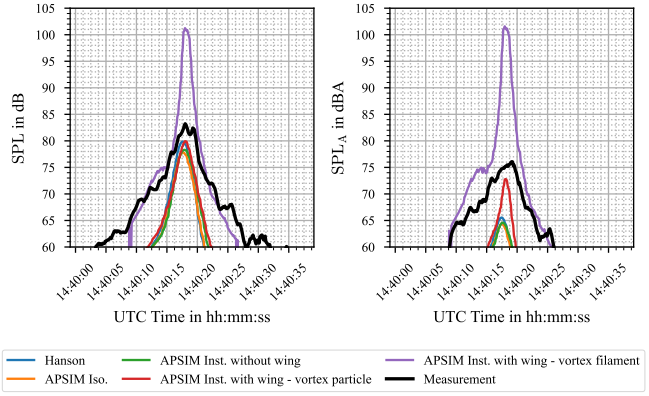

Figure 5: Level time history plot validating L_p values for isolated and installed propeller with fly-over data

The comparison in Fig. 5 reveals that for non-weighted plots, both isolated propeller simulated using VFM and installed propeller configurations using VPM simulations demonstrate good agreement with the measured data. However, installed configuration simulated using VFM overpredicts the noise levels by a range of 15 dB to 17 dB compared to VPM, which provides a closer match. In contrast, when considering A-weighted plots, the difference between the measured data and isolated propeller configurations simulated using the Hanson model and Formula 1A increases to a range of 10 dB to 12 dB.

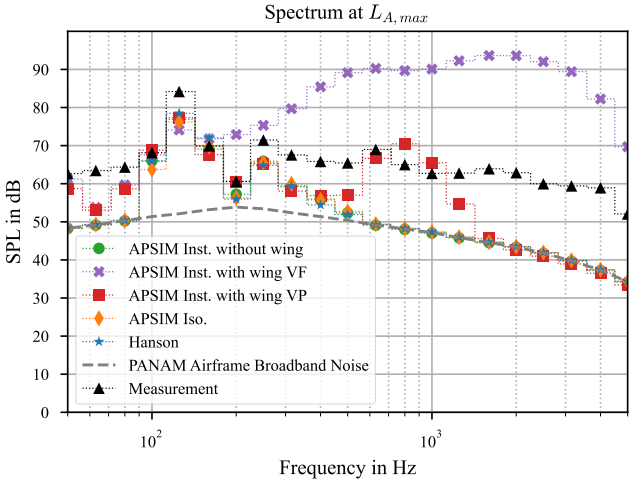

Figure 6: Spectrum plot validating L_p values for different propeller configuration to fly-over data

The discrepancy in A-weighting is attributed to its effect on low-frequency tones, which are suppressed, and mid-frequency harmonics, which are amplified. While VFM simulations exhibit increased noise levels after the second blade pass frequency due to panel wake development, VPM offers a more accurate representation of the noise levels, particularly in capturing the interaction effects and closely matching the measured data up to 1 kHz frequency as shown with the spectrum plot in Fig. 6. The reason for this deviation is that VFM fails to adhere to the tangential flow boundary conditions at collocation points, causing the wake from the propeller to enter the wing surface and interact with the doublet singularities defined at the camber of the airfoil. This leads to increased noise levels, as described in detail by Manghnani *et al.* [1], and shown in Figs. 5 and 6. Conversely, VPM applies boundary conditions to each particle, preventing it from interacting with the wing surface and resulting in a more accurate simulation.

Given these findings, VFM is recommended for cases where there is no interaction between the propeller wake and source/doublet singularities, such as the wing, due to its computational efficiency. In contrast, VPM is preferred for scenarios involving wake-structure interaction due to its capabilities to handle interaction effects.

Reduced order modeling

Mathematical domain for ML model

Following successful validation of results from the propeller noise source model, coupled with the FW-H equation solver, the next step involves down-selecting parameters that significantly influence the noise emitted to the far-field. The parameters selected for the reduced order model (ROM) are specified in Table 1, which is limited to single diameter propellers and constant angle of attack due to simplification to facilitate computationally efficient analysis. A sensitivity study was conducted to identify the most influential factors, resulting in this down-selected dataset.

Table 1: Parameter selected for reduced order model

Parameters	Range
Angle of Attack	[0.0]
Propeller Diameter	[2.5]
Wing Thickness	[0.8, 1.0, 1.2]
Number of blades	[3, 4, 5, 6]
Propeller RPM	[1300.0 ... 2000.0]
Propeller blade pitch	[0.0 ... -20.0]
Flight velocity (Knots)	[100.0 ... 200.0]
x-installed distance	[0.2 ... 0,8]
y-installed distance	[0.0]
z-installed distance	[-0.5 ... 0.5]

To create a comprehensive dataset, a generic geometry for a propeller installed with a wing is defined as shown in Fig. 7. The Dornier DO-228 propeller and wing geometry are used, but the sweep of the wing is eliminated to adopt a simplified box-shaped design with constant thickness and chord length throughout its span. The DO-228

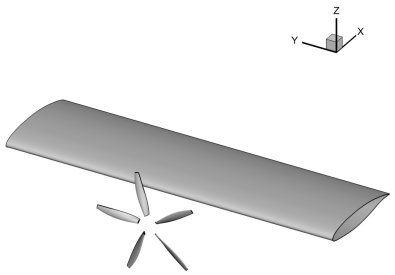

Figure 7: Generic geometry of propeller installed with the wing

wing airfoil is employed to create this generic test case, ensuring accurate representation of the wing's aerodynamic properties. The installation distance in longitudinal, lateral, and vertical directions is set at $x = 0.9$ m, $y = 2.55$ m, and $z = 0.35$ m, which matches the installation location of the propeller in the actual aircraft geometry. This configuration serves as the reference for further testing with random test points generated inside the computational domain using Halton sampling.

The test points are generated to cover the entire mathematical domain, including boundary points, to ensure a comprehensive representation of the effects of various parameters on propeller noise emission. The dataset characteristics include five parameters defined in continuous space and two parameters: number of propeller blades (B) and wing thickness ($\frac{t}{C}$), defined in discrete space. This is done to accommodate enough cases for different numbers of propeller blades while maintaining computational efficiency by avoiding the generation of panel mesh for the wing geometry for each case. The dataset is created based on Halton sampling inside the mathematical domain defined, resulting in a comprehensive set of data to study the effects of various parameters on propeller noise emission.

Future work will focus on expanding the dataset by incorporating variations in propeller diameter, sweep angle, and twist, allowing for comprehensive analysis of different propeller geometries under various operating conditions. Additionally, exploring distinct angles of attack for both installed and isolated propellers will help model ground noise emissions during takeoff and landing phases.

Data-Driven Machine Learning model

The final step in developing a data-driven machine learning model involves formulating a mathematical function to predict aircraft propeller noise. This function depends on parameters listed in Table 1 and the noise directivity on an acoustic hemisphere, defined using a virtual microphone grid with polar angles (Θ) ranging from 10° to 170° and azimuthal angles (Φ) ranging from −90° to 90°, as shown in Fig. 1. Due to wing-wake interactions and propeller backloading, the noise directivity exhibits azimuthal asymmetry for installed propeller configurations.

The data output from the aeroacoustic simulations are processed and stored in look-up tables, with the first five SPL harmonics obtained via the Farassat 1A solution.

A supervised learning model is trained on this dataset, employing a fully connected neural network (FCNN) for regression. The FCNN maps input parameters to SPL values using multiple layers of weighted neurons. Regularization (L2) prevents overfitting, while an adaptive learning rate with exponential decay ensures stable convergence. The Adam optimizer is used to capture complex, nonlinear patterns arising from wing-wake interactions, and min-max scaling normalizes SPL values to improve training efficiency.

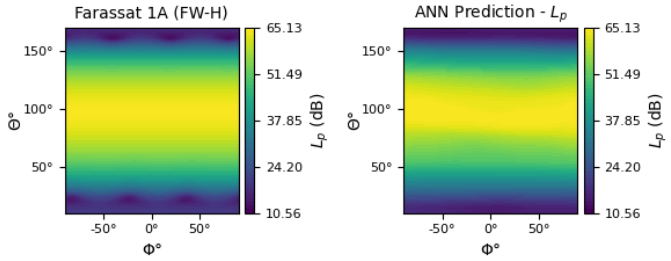

Figure 8: Isolated propeller: comparison of SPL values for Farassat 1A and ANN predictions

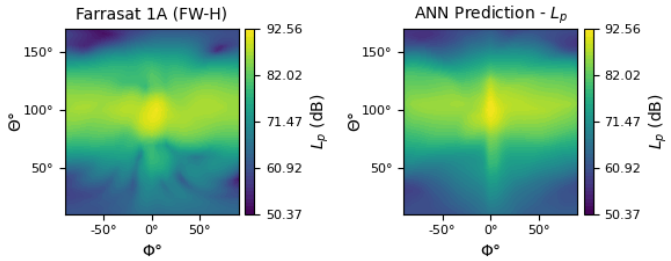

Figure 9: Installed propeller: comparison of SPL values for Farassat 1A and ANN predictions

Figs. 8 and 9 compare Farassat 1A and ANN-predicted SPL values for isolated and installed propeller cases. The ANN accurately captures noise directivity trends, with deviations at the microphone directly below the propeller (Φ=0° and Θ=90°) within 1 dB to 3 dB for both configurations. For the isolated case, the ANN correctly predicts azimuthal symmetry but does not reproduce numerical interference patterns at the hemisphere's edges, as these are filtered out by the weighting function. In the installed configuration, the AI model captures the loss of azimuthal symmetry but smooths out pressure fluctuations from wing-wake interactions, missing fine-scale variations present in the Farassat 1A solution.

Conclusion

This study concludes that the AI model, trained on data from a first-principles-based panel method (UPM) simulations coupled with the FW-H equation based solver (APSIM) using Formulation 1A from F. Farassat, accurately predicts first five SPL values and noise directivity trends in the far field for both isolated and installed propeller configuration. As a next step, the dataset will be expanded to include variations in diameter, sweep, twist, and angle of attack. The model will also be retrained using data from high-fidelity simulations and wind tunnel and fly-over measurements to further improve prediction accuracy.

Acknowledgment

The authors gratefully acknowledge the scientific support and HPC resources provided by the German Aerospace Center (DLR). The HPC system CARA is partially funded by "Saxon State Ministry for Economic Affairs, Labour and Transport" and "Federal Ministry for Economic Affairs and Climate Action". The HPC system CARO is partially funded by "Ministry of Science and Culture of Lower Saxony" and "Federal Ministry for Economic Affairs and Climate Action". Furthermore, the authors would like to thank Vincent Domogalla from DLR AS-HEL Göttingen for his contribution to the work.

References

[1] Manghnani, J., Domogalla, V., Ewert, R., Bertsch, L., Delfs, J .: A First Principle Based Approach for Prediction of Tonal Noise From Isolated and Installed Propeller 30th AIAA/CEAS Aeroacoustics Conference (2024), 10.2514/6.2024-3382

[2] Farassat, F..: Derivation of Formulations 1 and 1A of Farassat, NASA Langley Research Center, 2007, https://ntrs.nasa.gov/citations/20070010579

[3] Delfs, J. W., and Yin, J., .: Improvement of DLR Rotor Aeroacoustics Code (APSIM) and its Validation with Analytical solutions European Rotorcraft Forum, Vol. 29, 2003, https://dspace-erf.nlr.nl/server/api/core/bitstreams/508342ce-00f7-4a6b- 8be9-7a924e711398

[4] Ahmed, S. R., and Vidjaja, V. T.: Unsteady panel method calculation of pressure distribution on BO 105 model rotor blades Journal of American Helicopter society, Vol. 1, No. 43, 1998, pp. 47–56. https://doi.org/10.4050/JAHS.43.47.

[5] Feldhusen-Hoffmann, et. al. .: Noise and local pollutants of small aircraft: overview of simulation activities and of the first flight test within the DLR project L2INK AIAA AVIATION 2023 Forum, American Institute of Aeronautics and Astronautics, Reston, Virginia, United States, 2023. https://doi.org/10.2514/6.2023-4171.

[6] Weinke, F and Bertsch, L and Iwanitzki, M and Balack, P and Häßy, J .: System noise assessment of conceptual tube-and-wing and blended-wing-body aircraft designs AIAA Aviation Forum, pages: 4170, doi:10.2514/6.2023-4170

[7] Hanson, Donald B.: Helicoidal Surface Theory for Harmonic Noise of Propellers in the Far Field AIAA Journal, 1980, pages: 1213-1220, issn: 0001-1452, doi: 10.2514/3.50873